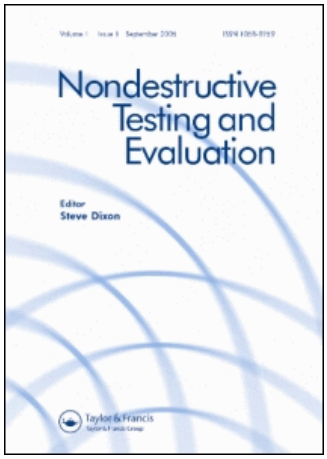

Nondestructive Testing and Evaluation
Publication details, including instructions for authors and subscription information:
http://www.informaworld.com/smpp/title~content=t713645777

Quantitative evaluation of discrete failure events in composites using infrared imaging and acoustic emission

Harry I. Ringermacher [a]; Bryon Knight [a]; Jian Li [a]; Yuri A. Plotnikov [a]; Gulperi Aksel [a]; Donald R. Howard [a]; Jeffry L. Thompson [a]
[a] General Electric Global Research Center, Schenectady, NY, USA

Online Publication Date: 01 June 2007
To cite this Article: Ringermacher, Harry I., Knight, Bryon, Li, Jian, Plotnikov, Yuri A., Aksel, Gulperi, Howard, Donald R. and Thompson, Jeffry L. (2007) 'Quantitative evaluation of discrete failure events in composites using infrared imaging and acoustic emission', Nondestructive Testing and Evaluation, 22:2, 93 - 99
To link to this article: DOI: 10.1080/10589750701447805
URL: http://dx.doi.org/10.1080/10589750701447805

Nondestructive Testing and Evaluation,
Vol. 22, Nos. 2–3, June–September 2007, 93–99

Taylor & Francis
Taylor & Francis Group

Quantitative evaluation of discrete failure events in composites using infrared imaging and acoustic emission

HARRY I. RINGERMACHER*, BRYON KNIGHT, JIAN LI, YURI A. PLOTNIKOV, GULPERI AKSEL, DONALD R. HOWARD and JEFFRY L. THOMPSON

General Electric Global Research Center, Schenectady, NY 12309, USA

We describe the successful synchronization of thermal imaging with acoustic emission to observe and characterize for the first time the thermal responses of discrete fiber breaks and matrix cracks in composite panels under load in real time. These events can be accurately described by ideal buried point and line thermal sources.

Keywords: Thermography; Acoustic emission; Composite failure; Transient infrared

1. Introduction

Transient infrared (IR) testing is performed on composite structures using traditional flash IR inspections to locate flaws and measure their depth. The method described here uses the "inflection point" approach of TTOF transient imaging (Ringermacher and Howard 2001), but instead of using flash lamps to apply a heat pulse, the heat is generated by the failure mode itself. From this prospective it borrows from the thermo-elasticity technique (Lesniak *et al.* 1997), where IR images of a fatigue crack are acquired from a dynamically loaded specimen. Failure modes in composite materials can be fiber breaks, matrix cracks or delaminations.

In traditional transient IR, the onset of the heat pulse is time zero for the event. However, because this method uses the heat generated by the failure mode, time zero is unknown to the IR system. To locate the thermal event zero-time, acoustic emission (AE) has been employed (Lesniak *et al.* 1997). When a thermal event occurs, whether it is a fiber break, matrix crack or a delamination, an AE event can be heard as well. A typical thermal response is shown schematically in figure 1. Here, the AE event has been used as the time zero to measure the thermal time-of-flight (Ringermacher *et al.* 1998) of the event. The thermal time-of-flight is measured at the inflection point (or point of maximum slope) of the thermal response, shown as τ in figure 1. The depth of the event can be calculated from τ and the thermal diffusivity.

*Corresponding author. Email: ringerha@crd.ge.com

Nondestructive Testing and Evaluation
ISSN 1058-9759 print/ISSN 1477-2671 online © 2007 Taylor & Francis
http://www.tandf.co.uk/journals
DOI: 10.1080/10589750701447805

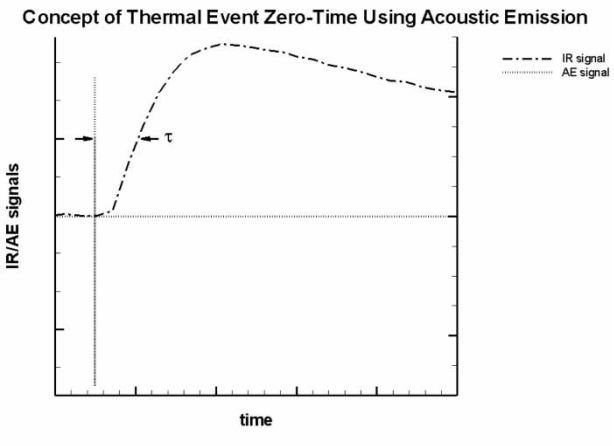

Figure 1. Concept of locating initiation of a thermal event (zero-time) using AE.

2. Theory—buried thermal sources

The sources for the buried thermal events in this work are very close to ideal. A fiber break, releasing significant energy, is essentially instantaneous and occurs at a point. It can, therefore, be modeled as an instantaneous point source. A matrix crack is not instantaneous but propagates along a line rapidly in a time much less than the characteristic time (thermalization time) for heat propagation in the z-direction. Thus it can be modeled as an instantaneous line source. The same is true for a propagating delamination zone, which can then be modeled as an instantaneous plane source. Point events are intralaminar. Line events will generally be confined to a single layer due to different bounding layer orientations.

The source model is shown in figure 2. The source is at $\{x', y', z'\}$. The response is observed at $\{x, y, z\}$. The Green's function solution for an instantaneous point source of unit strength at location $\{x', y', z'\}$, bounded between $z = 0$ and $z = l$, and observed at $\{x, y, z\}$ is

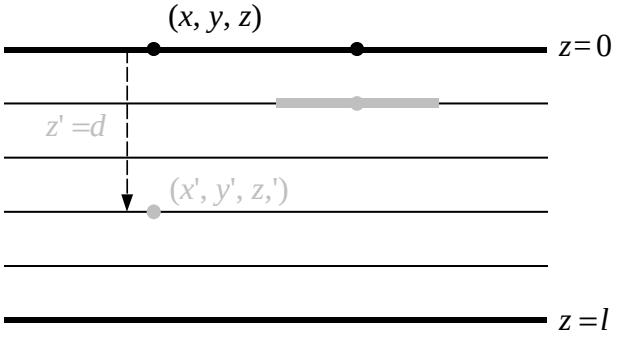

Figure 2. Source model.

given in Carslaw and Jaeger (1959),

$$T(x,y,z,t)=\frac{1}{4\pi l\alpha t}\mathrm{e}^{-((x-x')^2/4\alpha_x t)+((y-y')^2/4\alpha_y t)}\left(1+2\sum_{n=1}^{\infty}\mathrm{e}^{(-n^2\pi^2\alpha_z t)/l^2}\cos\left(\frac{n\pi z}{l}\right)\cos\left(\frac{n\pi z'}{l}\right)\right) \tag{1}$$

where, $\alpha=\sqrt{\alpha_x\alpha_y}$.

The anisotropic thermal diffusivities $\{\alpha_x, \alpha_y, \alpha_z\}$ typical of composite materials have been included. Line sources are obtained by integrating equation (1) along "y" from $-\infty \rightarrow +\infty$

$$T(x,z,t)=\frac{1}{2l\sqrt{\pi\alpha_x t}}\mathrm{e}^{-((x-x')^2/4\alpha_x t)}\left(1+2\sum_{n=1}^{\infty}\mathrm{e}^{(-n^2\pi^2\alpha_z t)/l^2}\cos\left(\frac{n\pi z}{l}\right)\cos\left(\frac{n\pi z'}{l}\right)\right) \tag{2}$$

where it has been assumed that the line source propagation distance is very much greater than its depth. Plane sources are obtained by integrating equation (2) along "x" from $-\infty \rightarrow +\infty$. The result is seen in equation (3).

$$T(z,t)=\frac{1}{l}\left(1+2\sum_{n=1}^{\infty}\mathrm{e}^{(-n^2\pi^2\alpha_z t)/l^2}\cos\left(\frac{n\pi z}{l}\right)\cos\left(\frac{n\pi z'}{l}\right)\right) \tag{3}$$

In each case the observation point of the event was at its epicentre $\{x=x', y=y', z=0\}$ as infrared emission $T(t)$, thus anisotropy has no effect on these waveforms and only the "z" thermal diffusivity plays a role. These three functions, resulting from equations (1–3), are shown plotted in figure 3. The definition of "unit strength" in a thermal Green's function refers to unit temperature density. Thus for a point "unit temperature" source this means (1/volume) while for a line and plane source this means (1/area) and (1/length) respectively. Scaling actual source temperature requires knowledge of the actual physical extent of the event. Since the energy content of the events can be dramatically different (e.g. a fiber break vs. a matrix crack), this is a difficult problem. Thus figure 3 is simply normalized to unity,

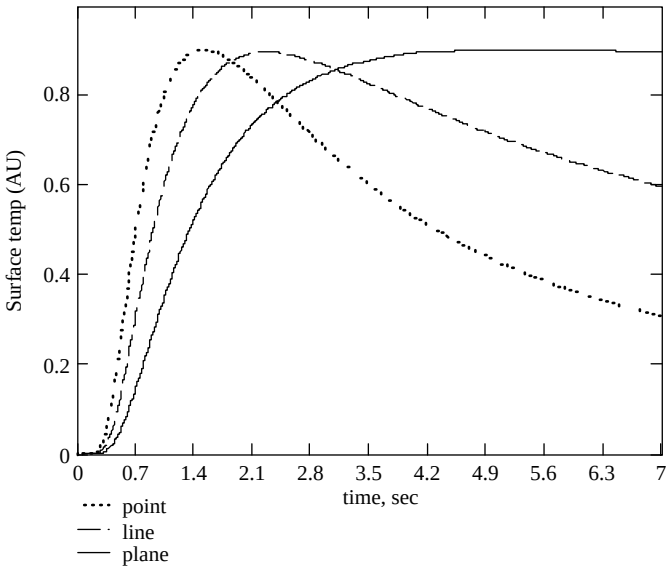

Figure 3. Epicentral thermal responses of ideal buried point, line and plane sources.

meaning equal surface temperature for all three sources—for clarity. In principle, further study would permit an estimate of the relative intensities of the events. It may be that a fiber break and matrix crack are "universal events" and have a nearly constant associated energy, which would be an interesting finding. In practice, the "inflection point" time (from the AE) and the peak temperature time (from the IR) are used to fit the data curves shown in later figures.

The locations of the inflection point on the time–temperature curve for each of the three sources is easily calculated from the point in time of maximum slope of the thermal response. The results are shown for, a point, a line and a plane from left to right:

$$\text{Point} : t_{\text{inflection}} = \frac{0.60\, d^2}{\pi^2 \alpha_z}, \quad \text{Line} : t_{\text{inflection}} = \frac{0.72\, d^2}{\pi^2 \alpha_z}, \quad \text{Plane} : t_{\text{inflection}} = \frac{0.9055\, d^2}{\pi^2 \alpha_z} \tag{4}$$

The plane source inflection point is in agreement with previous independently derived results (Ringermacher *et al.*1998) lending credence to this approach. The arrival time of the inflection point can be used to determine the depth, d, of the event as long as it is recorded at its epicenter, the centremost point of the observed infrared response.

3. Experimental set-up

The experimental system used to make the measurements consists of the IR camera system, the AE system and the load cell. The IR system used to collect the thermal data is an Indigo Phoenix DAS LWIR that has a 320 × 256 QWIP fpa. This is connected to a PC, which saves the raw thermal data from the IR camera system. A four-channel AE system is utilized to capture the acoustic signals released by each crack initiation event. The AE system runs four-channels simultaneously, including 100 KHz high-pass filters, 30 dB pre-amplifiers and a four-channel 10 MHz A/D converter. A 100Kip MTS servohydraulic test system with hydraulic wedge grips was used to apply the desired loading. The load was increased at a linear rate until the sample failed. Samples were stressed while IR data and AE data was simultaneously acquired. The samples used in the experiment were 20 ply graphite epoxy composite plates 12.7 cm wide by 50.8 cm long and 3.76 mm thick. Each sample has a slot machined in the centre of the plate that is 25.4 mm long and 6.35 mm in height. The setup is shown in figure 4 and is further described in Knight *et al.* (2006).

4. Data collection and analysis

For the sample test, four 200 KHz AE transducers were mounted on the same side of the sample that the IR camera was viewing. Due to the high speed of propagation of the acoustic signal compared to heat transfer, the ultrasonic transducers can pick up the acoustic signals within 50 μs after the initiation of the crack. For each signal event, the system automatically records the waveform for 200 μs. Each waveform file is time-stamped by the AE system with an accuracy of 5 μs. This accuracy is sufficient for the synchronization with the IR camera because the timing resolution of the latter is 20 ms. The IR data was collected using

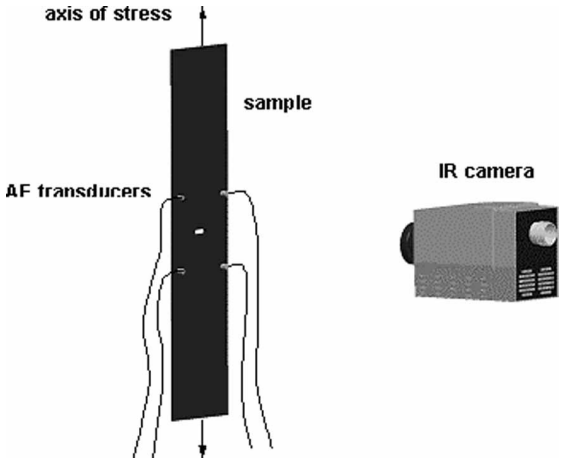

Figure 4. Set-up showing camera orientation with respect to AE transducers and notch.

a frame-rate of 52 fps at an integration time of 16 ms and a frame size of 320 × 256 pixels for a period of 6000 frames. In order to synchronize the IR and AE data a standard pencil lead break was used. The timing of the AE signal acquired as a result of the pencil lead break and the time at which the lead break is seen in the IR image is used to set a common event in the time bases of each of the systems. The procedure used to analyse the data consists of reviewing the raw IR data and choosing events with high thermal responses. Each of these events was then correlated with its corresponding AE event. The depth of the event was then calculated based on the type of failure mode using equations (4).

5. Results and discussion

Observed data were fitted best to either a point or a line source. Plane sources were not observed. The nature of the source could be clearly seen on the surface as either point-like or line-like. Typical images of a point source and line source are shown in figure 5.

These events occur in the vicinity of the notch. The line events always seem to occur in 45° plys. The time of the relevant AE event, as described earlier, was taken as the zero-time for

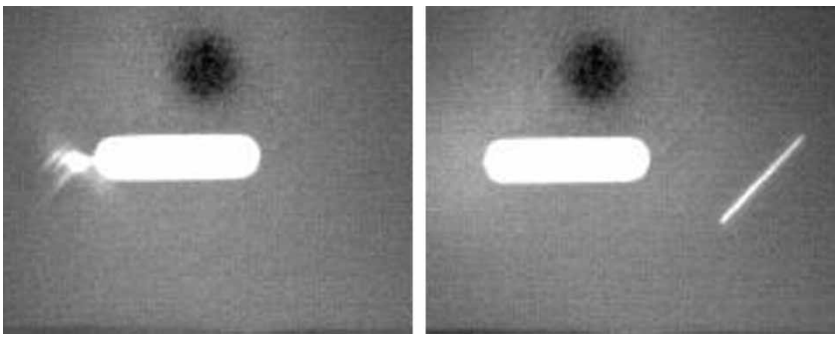

Figure 5. Infrared image of a buried point source at ply 10 (left) showing on the surface as a hot spot to the left of the notch and a buried line source at ply 3 (right). Additional small events are seen near the high-intensity point source releasing heat along the 45° ply.

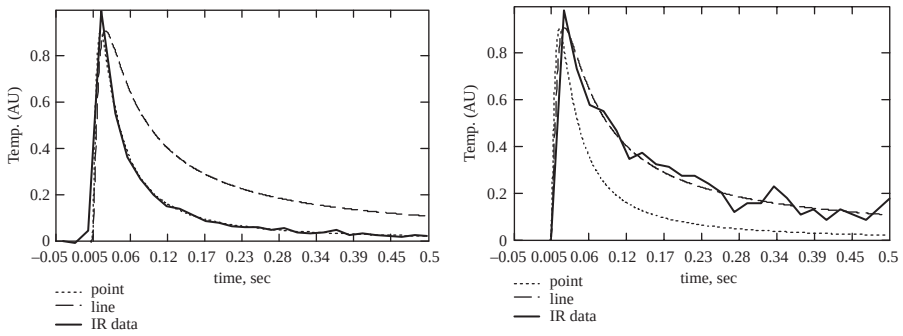

Figure 6. Epicentral thermal responses of observed buried point source (left) and line source (right) at a depth of 1 ply.

the buried thermal event. The inflection time was then easily determined from equation (4). The appropriate fit to either a point or line event always agreed with the corresponding measured inflection time for the point or line event at the evaluated depth. Thus there was double confirmation for the event location: (1) the predicted inflection time agreed with the measured inflection time for the type of event (point or line) at depth, d; and (2), the best fit to the event agreed with the observed shape at depth, d. Figure 6 shows the responses and fits for a buried point source (fiber break) and line source (matrix crack) at a depth of 1 ply. The predicted inflection times were 5.5 and 6.6 ms, respectively. It was apparent by observation that these were "ply-1" events since the rise times could not be resolved due to the camera speed resolution of 20 ms. Thus these inflection points could not be measured. The fits are excellent for the 1 ply depth. Figure 7 shows the responses and fits for a buried point event at a depth of 10 plies (figure 5, left) and line event at a depth of 3 plies (figure 5 right). The predicted and measured inflection times for the deep point event and shallow line event are in good agreement and the results can be seen in table 1.

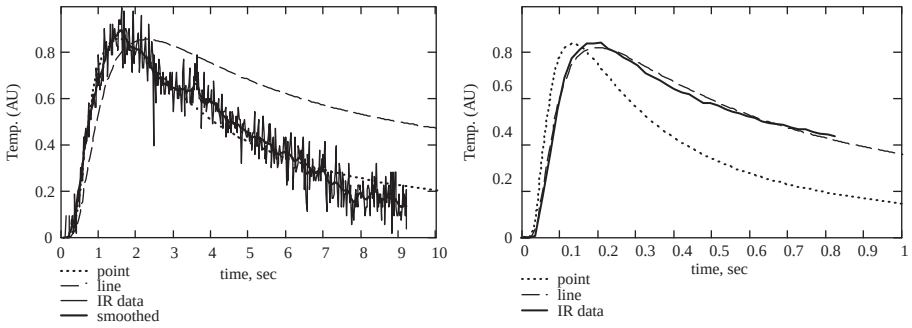

Figure 7. Epicentral thermal responses of a buried deep point event (left) and a line event (right).

Table 1. Calculated and experimentally measured thermal time-of-flight for an observed buried deep point event and a line event.

	Measured τ *(s)*	*Calculated* τ *(s)*
Buried point source at ply 10 (fiber break)	0.55 ± 0.15	0.55
Buried line source at ply 3 (matrix crack)	0.060 ± 0.010	0.057

6. Conclusion

Infrared imaging has been successfully synchronized with AE sensing to measure the depth of discrete events including fiber breaks and matrix cracks associated with known failure modes in composite materials under load. Thus, for the first time, the exact coordinate location of a discrete event associated with failure has been determined. With sufficient statistics, such events can be correlated and compared with predicted failure mechanisms to confirm theoretical composite performance.

References

Carslaw, H.S. and Jaeger, J.C., *Conduction of Heat in Solids*, 1959 (Oxford University Press: London).

Knight, B., Ringermacher, H.I., Li, J., Plotnikov, Y.A., Aksel, G., Howard, D.R. and Thompson, J.L., Synchronization of infrared imaging with acoustic emission for measurement of discrete failure events in composites. In *Review of Progress in Quantitative Nondestructive Evaluation 26*, AIP Conference Proceedings edited by D.O. Thompson and D.E. Chimenti, 2006 (American Institute of Physics: Melville, NY).

Lesniak, J.R., Bazile, D.J., Boyce, B.R., Zickel, M.J., Cramer, K.E. and Welch, C.S., Stress intensity measurement via infrared focal plane array. *Proceedings of ASTM Non-traditional Methods of Sensing Stress, Strain and Damage in Materials and Structures*, 1997 (STP 1318: Philadelphia).

Ringermacher, H.I., Systems and method for locating failure events in samples under load, GE-RD213969-1, 2006, Patent Pending.

Ringermacher, H.I. and Howard, D.R., Synthetic thermal time-of-flight (STTOF) depth imaging. *Rev. Progr. Quant. Nondestruct. Eval.*, 2001, **20**, 487–491.

Ringermacher, H.I., Mayton, D.J., Howard, D.R. and Cassenti, B.N., Towards a flat-bottom hole standard for thermal imaging. In *Review of Progress in Quantitative Nondestructive Evaluation 17*, edited by D.O. Thompson and D.E. Chimenti, pp. 425–429, 1998 (Plenum Press: New York, NY).